ADAPTIVE DISTANCE PROTECTION FOR MULTI-TERMINAL LINES CONNECTING CONVERTER-INTERFACED RENEWABLE ENERGY SOURCES

Subhadeep Paladhi[1]*, Qiteng Hong[1], Campbell D. Booth[1]

[1]*Department of Electronic and Electrical Engineering, University of Strathclyde, Glasgow, United Kingdom*
*Email: subhadeep.paladhi@strath.ac.uk

Keywords: Distance relaying, multi-terminal lines, renewable energy sources, power system faults, zone-1 setting

Abstract

Variation in infeed current challenges the distance relay performance significantly for protection of multi-terminal lines. Underreach issue with such a line configuration becomes more prominent for a relay at the substation when connected to renewable sources, due to generation variability and converter control operation. This may result in an incorrect decision by the distance relay, especially with a fixed zone-1 setting. In this paper an adaptive distance relaying method is proposed for such line configurations. The method obtains the remote end data during pre-fault and calculates the fault distance to derive accurate protection decision. Performance of the proposed method is tested for a three-terminal line using PSCAD/EMTDC. Comparative assessment with conventional distance relaying demonstrates the superiority of the proposed method.

1 Introduction

Power grids are integrating renewable energy sources (RESs) in large scale to achieve the target of zero carbon emission [1]. Multi-terminal line configurations are common for such integration to exploit both technical and economic benefits [2], [3]. Underreach of distance relay is a generic issue with such line configuration [3]. Relays may become more vulnerable in the presence of RESs due to the high source-impedance-ratio and dynamic fault response of the interfacing converters [4]. Severe underreach vanishes the zone-1 overlapping region of the terminal distance relays [2]. This may even result in failure of communication assisted tripping schemes, commonly used for protecting lines with such configurations [5]. Generation variability, dynamic control operation and frequent amendments in grid code requirements ask for a revisit to the distance relay performance for multi-terminal lines in the presence of RESs.

High voltage multi-terminal lines are generally protected by distance and differential relaying schemes [3]. Differential protection is preferred over distance relaying for secure protection, but the scheme requires synchronized fault data from the remote end and also gets affected due to current transformer (CT) saturation [5], [6]. Different methods are available to ensure correct distance relay operation for protecting multi-terminal lines. An agent based adaptive distance relay setting technique is provided in [7] using available communication facilities. Several schemes are available in [8]–[12] which applies synchronized or unsynchronized voltage and current measurements of all terminals to identify fault location in a multi-terminal lines. The methods either consider the system to be homogeneous or show limited performance in cased high fault resistance and wide variation in system conditions. Methods using synchronized measurements from remote end during fault may delay the protection decision due to communication latency. Communication assisted tripping schemes employing distance

relaying decision of all terminals are common for such line configurations. Permissive overreach transfer trip (POTT) and directional comparison blocking (DCB) schemes use distance relay zone-2 decisions. These scheme are vulnerable to power swing, load encroachment and outfeed issues [3], [5]. Adaptive zone-1 setting based direct underreaching transfer trip (DUTT) proposed in [5] only considers three phase faults. Its performance will be under scrutiny for high resistance asymmetrical faults and system non-homogeneity in the presence of RESs. Schemes employing wavelet transform are proposed in [13]–[15] for protection of multi-terminal lines. Complexity in hardware implementation and extraction of frequency dependent information are the major issues for such schemes. Therefore, an improved technique is required for protection of multi-terminal lines to avoid all such limitations, especially in the presence of RESs.

This paper proposes an adaptive distance relaying method for protection of multi-terminal lines. The method obtains voltage and current data during prefault to calculate the infeed current during fault and determines actual fault distance to derive correct decision. Performance of the proposed method is tested for a three-terminal line simulated in PSCAD/EMTDC software platform. Results demonstrate the applicability of the proposed method with variation in fault resistance, grid code requirements, RES output and types of RESs.

2 Test System

A 400 kV three-terminal line, as shown in Fig. 1, is simulated in PSCAD/EMTDC software platform to demonstrate the issue and verify the performance of the proposed method. Unequal branch lengths are considered for demonstrating the issue [5]. Voltage and current phasors are estimated using 1-cycle discrete Fourier transform. A 300 MW solar photovoltaic plant is integrated at bus P. The solar plant consists of multiple units and each unit is connected to the common coupling bus through the standard converter and transformer arrangement

[16]. The solar plant is controlled in synchronous reference frame with feed-forward compensation and generate balanced current even during asymmetrical faults [17]. Zone-1 of each end distance relay are set as indicated in Fig. 1. Employing zone-1 decision at each end a DUTT scheme is also implemented in the system using commonly available low-bandwidth communication channels. DUTT scheme ensures the generation of trip signal if any of the relays find the fault within its zone-1 reach.
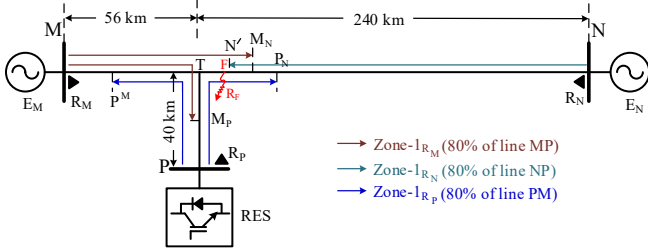

Fig. 1 Three-terminal line integrating RES to the grid and protected by distance protection scheme with DUTT.

3   Problem Statement

For a fault at F (adjacent to N'), apparent impedance calculated by the distance relay R_P at bus P is given by

$$Z_{app}^P = \frac{V_P^R}{I_P^R} = Z_{PF} + \left(\frac{I_M^R}{I_P^R}\right)Z_{TF} + \left(\frac{I_F}{I_P^R}\right)R_F. \tag{1}$$

Where V^R and I^R are the voltage and current measurements by the relay and may change with the fault types [4]. M, N and P in subscripts represent the corresponding measurement bus. I_F is the current through R_F. Thus Z_{app}^P includes an additional term $\left(\left(\frac{I_M^R}{I_P^R}\right)Z_{TF} + \left(\frac{I_F}{I_P^R}\right)R_F\right)$, which causes underreach/ overreach issue for the relay depending on the converter operation influencing phase angle of I_P^R. This may result in a malfunction of the distance relay R_P with fixed zone-1 setting at times. The overlapping region $N'P_N$ between zone-1 of relays R_P and R_N is required to ensure the correct operation of DUTT scheme, which can be calculated as in (2).

$$Z_{N'P_N} = 0.8Z_{PM} - (Z_{PT} + Z_{TN'}) \tag{2}$$

The DUTT scheme may also fail for a fault beyond N' (from bus N) if the underreaching impedance in (1) becomes higher than $Z_{N'P_N}$ or the relay R_P fails to detect the fault within its fixed zone1 setting due to severe overreach. Such limitations of available distance protection schemes is presented below for the system in Fig. 1. For the purpose, phase-A-to-ground (AG) and phase-B-to-phase-C-to-ground (BCG) faults are created at a distance of 225km from bus N with different fault resistances. The solar plant is complied with both European Union (EU) and North American (NA) grid codes at a time. EUGC prioritizes reactive power injection during fault, whereas NAGC compels the solar plant to maintain power factor close to unity even during fault. The faults are beyond the zone-1 reach of relay R_N. Results in Fig. 1 demonstrate that the apparent impedances calculated by R_P are also outside the zone-1 boundary due to underreach and overreach issues. Such issues ask for developing a new distance protection technique to ensure correct protection of multi-terminal lines.
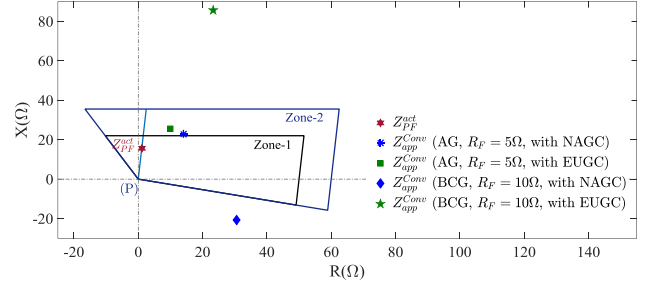

Fig. 2 Underreach and overreach performance of distance relay.

4   Proposed Method for Reliable Distance Protection Decision

The grid-feeding power converter connecting solar plant is generally modeled with a dependent current source in parallel with a high impedance [4]. At any particular instant, the current source can be converted to an equivalent voltage source (E_P) with a series impedance (Z_{SP1}) [18]. Z_{SP1} changes at each measurement instant, in accordance with the variation of solar irradiance, plant status and control operation.

With such a voltage source based representation an equivalent sequence network of the system in Fig. 1 is provided in Fig. 3 for an AG fault at F. Considering grid to be strong, the positive sequence model of other two sources are represented using voltage sources (E_M and E_N) with internal impedances (Z_{SM1} and Z_{SN1}) connected in series. Solar plant with feed-forward compensation generates balanced current even during asymmetrical faults. Therefore negative sequence circuit of the solar plant is represented with an open circuit.

As in (1), the apparent impedance calculated at T can be expressed as in (3).

$$\frac{|V_T^R|}{|I_T^R|}e^{j(\theta_V - \theta_I)} = |Z_{TF1}|e^{j\theta_{1L}} + \frac{|I_F|}{|I_T^R|}e^{j(\varphi - \theta_I)}R_F. \tag{3}$$

θ_V and θ_I are the phase angles of V_T^R and I_T^R. T . θ_{1L} and φ represent the phase angles of line impedance and the faulted path current respectively. (3) is rewritten in (4).

$$\frac{|V_T^R|}{|I_T^R|}e^{j(\theta_V - \varphi)} = |Z_{TF1}|e^{j(\theta_{1L} - \varphi + \theta_I)} + \frac{|I_F|}{|I_T^R|}R_F. \tag{4}$$

By separating the imaginary parts from both sides, (4) is rewritten in (5).

$$\frac{|V_T^R|}{|I_T^R|}\sin(\theta_V - \varphi) = |Z_{TF1}|\sin(\theta_{1L} - \varphi + \theta_I). \tag{5}$$

Thus $|Z_{TF1}|$ can be obtained from (5) as in (6).

$$|Z_{TF1}| = \frac{\frac{|V_T^R|}{|I_T^R|}\sin(\theta_V - \varphi)}{\sin(\theta_{1L} - \varphi + \theta_I)}. \tag{6}$$
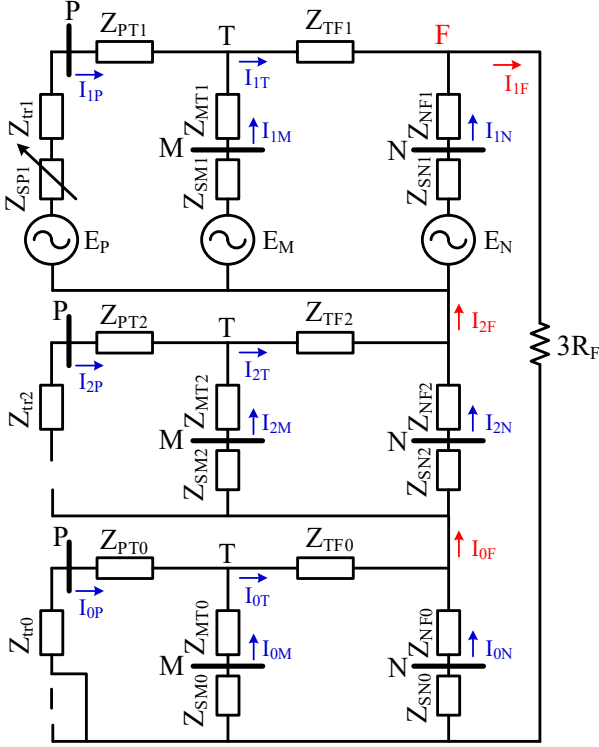
Fig. 3. Sequence network of the system in Fig. 1 for an AG fault.

For an AG fault, V^R and I^R can be replaced by V_A and $(I_A + K_0 I_0)$ respectively [4]. $K_0 = \left(\frac{Z_{0L} - Z_{1L}}{Z_{1L}}\right)$ is the zero sequence compensation factor. Thus the variables at T can be expressed as in (7).

$$V_T^R = V_{AT} = V_{1T} + V_{2T} + V_{0T}$$
$$I_T^R = I_{AT} + K_0 I_{0T} = I_{1T} + I_{2T} + (1 + K_0) I_{0T} \qquad (7)$$

Applying voltage drop principle, V_T^R can be obtained as,

$$V_T^R = (V_{1P} - I_{1P} Z_{PT1}) + V_{2P} + (V_{0P} - I_{0P} Z_{PT0}). \qquad (8)$$

Z_{SM1} can be computed using multiple voltage and current measurements at M during pre-fault, as in [19]. Similarly, Z_{SM2} and Z_{SM0} can be computed for a previous unbalanced fault situation. Even with circuit breaker status and system impedance data, these impedances can be computed at M and updated with time.
I_T^R is the combined fault current contribution from bus M and P. Thus I_T^R in (7) can be rewritten as,

$$I_T^R = (I_{1M} + I_{1P}) + I_{2M} + (1 + K_0)(I_{0M} + I_{0P}) \qquad (9)$$

Using Z_{SM1}, E_M is computed and updated at every computation instant. The internal voltage and sequence impedances are communicated to bus P during pre-fault, which are applied with the sequence voltages at T (as computed in (8)) to calculate the sequence currents from bus M as in (10).

$$I_{1M} = \frac{(E_M - V_{1P} + I_{1P} Z_{PT1})}{(Z_{SM1} + Z_{MT1})}$$
$$I_{2M} = \frac{-V_{2P}}{(Z_{SM2} + Z_{MT2})}, I_{0M} = \frac{(Z_{PT0} + Z_{tr0}) I_{0P}}{(Z_{SM0} + Z_{MT0})} \qquad (10)$$

Following computation of V_T^R and I_T^R, φ remains as the only unknown parameter required to determine $|Z_{TF1}|$ using (6). For AG fault, $I_{1F} = I_{2F} = I_{0F}$ (as shown in Fig. 3). RESs are generally connected to the grid through dYg transformer, which maintains the homogeneity in the zero sequence network. Thus φ for AG fault is obtained as in (11).

$$\varphi = arg(I_{0F}) = arg(I_{0P}) \qquad (11)$$

Similarly, φ for other types of faults is derived using corresponding sequence network. Thus the fault distance from T point is calculated accurately by dividing $|Z_{TF1}|$ by per-unit line impedance magnitude.

4.1 Implementation of proposed algorithm

Steps associated with proposed adaptive distance relaying scheme are provided in Fig. 4. Internal voltages and equivalent source impedances are estimated at the infeed end using pre-fault voltage and current measurements and the available system impedance data. The estimated data are communicated to the RES connected substation during pre-fault using available communication channel. Following detection and classification, the fault is checked whether it is within the T point from relay points or not for both RES connected bus and infeed bus, using the method in [4]. For a fault point beyond the T point from both the buses V_T^R and I_T^R are computed using (8) - (10). Phase angle of the faulted path (φ) is computed according to the fault type (as in (11) for AG fault). The faulted section impedance from T point ($|Z_{TF1}|$) is calculated following the computation of V_T^R, I_T^R and φ. Finally, a decision is derived based on the impedance from relay bus to fault point ($|Z_{PT1}| + |Z_{TF1}|$).
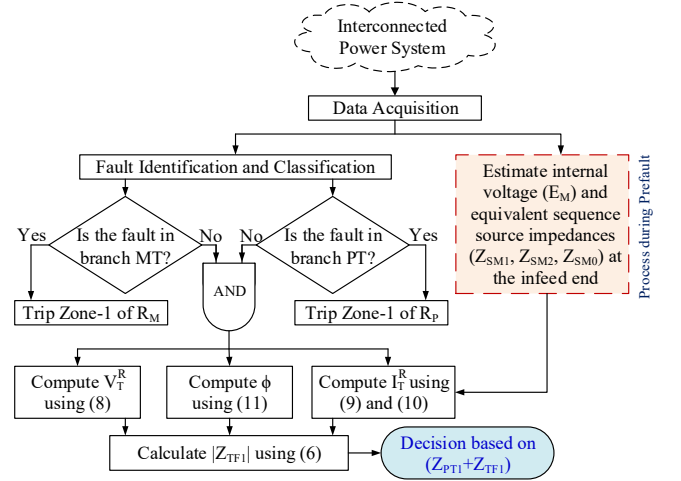

Fig. 4. Flow chart of the proposed protection scheme.

5   Results

Proposed protection method is tested for RES integrated three-terminal line of Fig. 1. Performance of the relay R_P at RES connected bus is evaluated for different faults with variation in fault resistance, RES generation, grid code compliance and types of RESs. Comparative assessment with conventional distance relaying technique is provided to demonstrate the strength of the proposed method. Positive and zero sequence

line impedances used in the system are $(0.02+j\,0.2867)$ Ω/km and $(0.106+j\,0.837)$ Ω/km respectively.

5.1 For different fault types and fault resistances

Fault severity changes with its type and associated fault resistance. Additional impedance associated with the apparent impedance in (1) varies accordingly. Converter control modulates the phase angle of the fault current at RES connected bus and results in underreach and overreach issues for the relay. This is demonstrated in Fig. 5. Fig. 5(a) shows the apparent impedances calculated by relay R_P for different types of faults, created in branch TN at a distance of 225km from bus N with $R_F = 5\Omega$. Fig. 5(b) provides the results where the performance of R_P is tested for BCG faults, created at same location in branch TN with variation in R_F. Results demonstrates that R_P fails to identify most of the faults with its fixed zone-1 setting. The faults being created at a distance beyond zone-1 reach of R_N, such situations also result in failure of DUTT scheme available for the system protection (as mentioned in Section II).
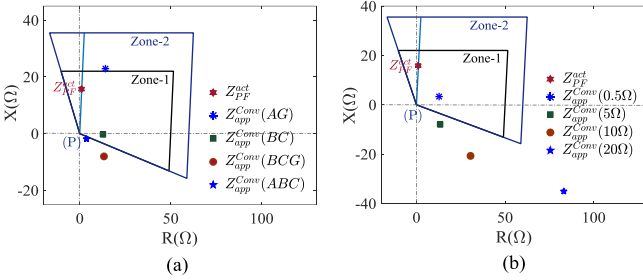

Fig. 5. Underreach and overreach performance of distance relay with change in (a) fault types and (b) fault resistances.

With the proposed scheme, the fault locations are first identified to be beyond the T point from both M and P buses individually, by applying the method in [4]. Relay R_P obtains the estimated source equivalent data at infeed bus M during pre-fault and computes the voltage and currents at T. Following the computation, the relay calculates the faulted section impedance from point T and takes the decision accordingly. The faulted section impedances calculated for all the above cases are provided in Column V (z_{PF}^{prop}) with some additional cases, which match exactly with the actual faulted section impedance data (z_{PF}^{act}). Shaded boxes in Column IV represents the maloperation of R_P with conventional approach. The results demonstrate the superiority of the proposed scheme over conventional distance relaying.

5.2 For RESs complied with different grid codes

Fault current angle of RES gets modulated with the applied grid code. This affects the underreach and overreach issue of distance relay in a multi-terminal line protection. Performance of both conventional and proposed distance relaying schemes are tested for R_P in the system of Fig. 1. Different fault cases are created in branch TN, at a distance of 225km from bus N, while the solar plant at P is complied with NAGC and EUGC (one at a time). Results are provided in Table II. This shows the adaptability of the proposed scheme in the presence of RESs with different grid code compliances.

Table 1. Performance evaluation for different types of faults with different fault resistances

Fault Type	R_F (Ω)	$Z_{PF}^{act} = Z_{PT}+Z_{TF}$		Z_{app}^{conv}		Z_{PF}^{prop}	
		R_{PF}^{act} (Ω)	X_{PF}^{act} (Ω)	R_{app}^{conv} (Ω)	X_{app}^{conv} (Ω)	R_{PF}^{prop} (Ω)	X_{PF}^{prop} (Ω)
AG	0.5	1.10	15.77	5.78	24.59	1.10	15.79
	5	1.10	15.77	14.01	22.84	1.10	15.83
	10	1.10	15.77	21.97	18.20	1.11	15.86
	20	1.10	15.77	16.15	15.09	1.11	15.92
BC	0.5	1.10	15.77	14.41	5.65	1.10	15.79
	5	1.10	15.77	12.67	-0.36	1.10	15.83
BCG	0.5	1.10	15.77	12.68	3.32	1.10	15.81
	5	1.10	15.77	13.25	-7.94	1.11	15.86
	10	1.10	15.77	30.61	-20.79	1.11	15.92
	20	1.10	15.77	83.01	-35.10	1.11	15.95
ABC	0.5	1.10	15.77	3.65	-0.90	1.10	15.81
	5	1.10	15.77	3.60	-1.84	1.11	15.89

Table 2. Performance evaluation in the presence of RESs complying with different grid codes

Fault (R_F)	Grid Code	Z_{PF}^{act}		Z_{app}^{conv}		Z_{PF}^{prop}	
		R_{PF}^{act} (Ω)	X_{PF}^{act} (Ω)	R_{app}^{conv} (Ω)	X_{app}^{conv} (Ω)	R_{PF}^{prop} (Ω)	X_{PF}^{prop} (Ω)
AG (5Ω)	NAGC	1.10	15.77	14.01	22.84	1.10	15.83
	EUGC	1.1	15.77	10.02	25.58	1.10	15.72
BCG (10Ω)	NAGC	1.10	15.77	30.61	-20.79	1.11	15.92
	EUGC	1.1	15.77	23.26	85.57	1.11	15.84

5.3 With variation in RES output

Generation variability is common with RES. This changes the source-impedance-ratio significantly at RES connected bus and affects the distance relay performance accordingly. Performance of R_P in Fig. 1 is tested for such situations with variation in solar plant output. AG faults with $R_F = 20\Omega$ and BCG faults with $R_F = 10\Omega$ are created in branch TN, at a distance of 225km from bus N. Results provided in Table III demonstrate that the apparent impedances calculated by the conventional distance relay vary significantly with variation in solar plant generation. Proposed method calculates the faulted section impedance accurately and results in correct protection decision for all the cases.

Table 3. Performance evaluation with variation in RES output

Fault (R_F)	PV output (%)	Z_{PF}^{act}		Z_{app}^{conv}		Z_{PF}^{prop}	
		R_{PF}^{act} (Ω)	X_{PF}^{act} (Ω)	R_{app}^{conv} (Ω)	X_{app}^{conv} (Ω)	R_{PF}^{prop} (Ω)	X_{PF}^{prop} (Ω)
AG (20Ω)	100	1.10	15.77	16.15	15.09	1.11	15.92
	75	1.10	15.77	38.14	18.25	1.11	15.92
	50	1.10	15.77	40.04	21.64	1.11	15.91
	25	1.10	15.77	41.88	25.44	1.11	15.90
BCG (10Ω)	100	1.10	15.77	30.61	-20.79	1.11	15.92
	75	1.10	15.77	52.07	-30.34	1.11	15.93
	50	1.10	15.77	87.56	-45.95	1.11	15.96
	25	1.10	15.77	186.31	-89.66	1.11	15.92

5.4 Performance with different RESs

Control operation varies significantly with change in RES types. This influences the performance of conventional distance relay significantly. Performance of relay R_P in such

4

situations are tested by replacing the solar plant at P with Type-III and Type-IV wind farms at a time. For the purpose, BCG faults are created in branch TN, at a distance of 225km from bus N with $R_F = 10\Omega$. Results shown in Fig. 1 demonstrate the wide variation in apparent impedance with change in RES type. It is observed that the relay applying proposed method calculates the faulted section impedances as $(1.11+j15.92)$ Ω, $(1.11+j15.84)$ Ω and $(1.11+j15.89)$ Ω with solar plant, Type-III and Type-IV wind farms respectively, which are close to the actual impedance value. Thus the proposed method derives correct protection decisions for all the cases. This demonstrates the proposed method to be independent of control operation associated with different RESs.
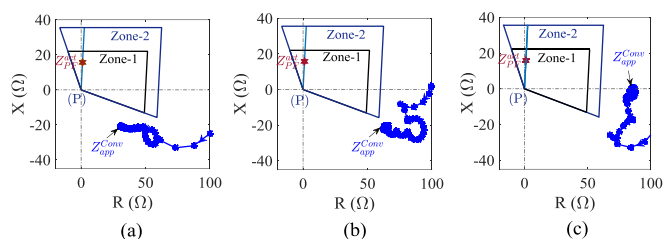

Fig. 6. Performance of conventional distance relaying for three-terminal lines integrating (a) solar plant, (b) Type-III wind farm and (c) Type-IV wind farm.

6 Conclusion

Underreach and overreach of distance relay due to infeed variation are the generic issues for multi-terminal line protection. Converter-based sources introducing high source-impedance-ratio makes the issues more prominent when integrated using such line configurations. Zone-1 overlapping may disappear between relays at times and result in malfunction of communication assisted schemes like DUTT. An adaptive distance relaying method is proposed for such line configurations. The method computes the sequence impedances and equivalent internal voltage at the infeed end during pre-fault and applies to compute correct fault distance. Accurate performance of the proposed method is demonstrated for a three-terminal line for different fault types and fault resistances. The method is also tested in the presence of different RESs complied with different grid codes, and with variation in RES output. Results demonstrate the superiority of the proposed method compared to conventional distance relaying approach.

7 Acknowledgement

8 References

[1] "Guidelines for implementation of scheme for setting up of 750 MW grid-connected solar PV power projects under batch-1," Jawharlal Nehru National Solar Mission, Ministry of New and Renewable Energy, New Delhi, India, Tech. Rep., October 2013, [Online]. Available: http://mnre.gov.in/file-manager/UserFiles/final-VGF750MW Guidelines for-grid-solar-power-projects.pdf.

[2] "IEEE guide for protective relay applications to transmission lines," IEEE Std C37.113-2015 (Revision of IEEE Std C37.113-1999, pp. 1–141, 2016.

[3] S. Protection and C. T. F. of the NERC Planning Committee, "The complexity of protecting three-terminal transmission lines," North American Electric Reliability Council, Tech. Rep., September 2006.

[4] S. Paladhi and A. K. Pradhan, "Adaptive distance protection for lines connecting converter-interfaced renewable plants," IEEE J. Emerg. Sel. Topics Power Electr., 2020 (to be published), available in early access.

[5] S. Sarangi and A. K. Pradhan, "Adaptive direct underreaching transfer trip protection scheme for the three-terminal line," IEEE Trans. Power Del., 2015, (30), 6, pp. 2383–2391.

[6] R. K. Aggarwal and A. T. Johns, "The development of a new high speed 3-terminal line protection scheme," IEEE Power Eng. Review, 1986, (6), 1, pp. 43–43.

[7] D. Coury, J. Thorp, K. Hopkinson, and K. Birman, "Agent technology applied to adaptive relay setting for multi-terminal lines," in 2000 Power Engineering Society Summer Meeting (Cat. No.00CH37134), vol. 2, 2000, pp. 1196–1201 vol. 2.

[8] Y.-H. Lin, C.-W. Liu, and C.-S. Yu, "A new fault locator for three-terminal transmission lines using two-terminal synchronized voltage and current phasors," IEEE Trans. Power Del., 2002, (17), 2, pp. 452–459.

[9] B. Mahamedi, M. Sanaye-Pasand, S. Azizi, and J. G. Zhu, "Unsynchronised fault-location technique for three-terminal lines," IET Gen., Trans. & Distr., 2015, (9), 15, pp. 2099–2107.

[10] P. K. Nayak, A. K. Pradhan, and P. Bajpai, "A three-terminal line protection scheme immune to power swing," IEEE Trans. Power Del., 2016, (31), 3, pp. 999–1006.

[11] S. Brahma, "Fault location scheme for a multi-terminal transmission line using synchronized voltage measurements," IEEE Trans. Power Del., 2005, (20), 2, pp. 1325–1331.

[12] V. K. Gaur, B. R. Bhalja, and M. Kezunovic, "Novel fault distance estimation method for three-terminal transmission line," IEEE Trans. Power Del., 2021, (36), 1, pp. 406–417.

[13] M. Eissa, "A new digital relaying scheme for EHV three terminal transmission lines," Electric power systems research, 2005, (73), 2, pp. 107–112.

[14] L. N. Tripathy, M. K. Jena, S. R. Samantaray, and D. R. Dash, "A differential protection scheme for tapped transmission line containing UPFC and wind farm," in Proceedings of the 2014 IEEE Students' Technology Symposium, 2014, pp. 319–324.

[15] B. Bhalja and R. Maheshwari, "New differential protection scheme for tapped transmission line," IET Gen., Trans. & Distr., 2008, (2), 2, pp. 271–279.

[16] C. Loutan, P. Klauer, S. Chowdhury, S. Hall, M. Morjaria, V. Chadliev, N. Milam, C. Milan, and V. Gevorgian, "Demonstration of essential reliability services by a 300-MW solar photovoltaic power plant," National Renewable Energy Lab.(NREL), Golden, CO (United States), Tech. Rep., 2017.

[17] S. Paladhi and A. K. Pradhan, "Adaptive fault type classification for transmission network connecting converter-interfaced renewable plants," IEEE Systems Journal, 2021, (15), 3, pp. 4025-4036.

[18] C. K. Alexander, Fundamentals of Electric Circuits. McGraw-Hill, 2009.

[19] S. Paladhi and A. K. Pradhan, "Resilient protection scheme preserving system integrity during stressed condition," IET Gen., Trans., Dist., 2019, (13), 14, pp. 3188–3194.